The Quantum World of Cold Electron Collisions

DAVID FIELD,* STUART L. LUNT, AND JEAN-PIERRE ZIESEL

Institute of Physics and Astronomy, University of Aarhus, DK-8000 Aarhus C, Denmark, and Laboratoire Collisions Agrégats Réactivité, Université Paul Sabatier, 31062 Toulouse, France

Received August 24, 2000

ABSTRACT

Collisions between electrons and molecules at thermal energy play a key role in the chemistry and physics of plasmas, ranging from those in space to the chemically active plasmas used for thin film and microcircuit fabrication. However, until recently, data for electron−molecule interactions below a few hundred millielectronvolts impact energy (a few thousand kelvin) were very sparse. Our experiments, using a high-resolution synchrotron photoionization source of electrons, have opened up this low-energy field. We present recent results which reveal some of the striking quantum scattering events which take place as long-wavelength, low-energy electrons encounter molecules, choosing H_2, N_2, benzene, halobenzenes, methanol, ozone, and chlorine dioxide as examples.

1. Introduction

The fall of sunlight upon the atmosphere of the earth, starlight upon the interstellar medium, or the simple act of turning on a light all lead to the formation of a gas plasma. In these plasmas are neutral atoms and molecules, positive and negative ions, and electrons. These species interact, forming a complex mixture whose nature may only be understood by detailed studies of the fundamental collision processes which take place. Among these processes, electron−molecule interactions are paramount. Despite their tiny momentum, low-energy electrons turn out to be very efficient in causing molecules to become rotationally, vibrationally, and electronically excited. Electron collisions may also cause molecules to dissociate into neutral and negative ion products. In other collisions, electrons may be deflected in their paths with negligible exchange of energy, a process which determines the rate of diffusion of electrons in gases. All types of events contribute to the properties of both natural and man-made plasmas, for example around hot stars, in quasars or in the early Universe, in our own upper atmosphere and other planetary atmospheres, in gas lasers, and in the chemically rich discharges used in industrial plasma processing. To give a single example, N_2 may become vibrationally excited in collisions with electrons and in a CO_2 laser transfer this excitation to CO_2, forming the population inversion necessary for laser action. The nature of electron−molecule scattering data is, in fact, nicely illustrated by the variation with electron impact energy of the scattering cross-section of electrons by N_2; data are shown in Figure 1. Vibrational excitation of N_2 by electron impact is associated with the strong resonant structure between 2 and 3 eV. Recent results have revealed the importance of low-energy scattering in biological material.[1] Secondary electrons, released by ionizing radiation falling upon cells, cause efficient bond breakage in DNA, data which give new impetus to the study of low-energy electron collisions.

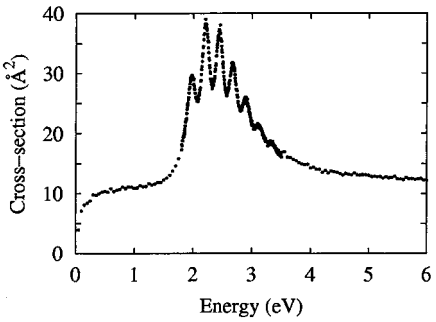

FIGURE 1. Variation with electron energy of the electron-scattering cross-section integrated over all angles for all elastic and inelastic processes (the "total integral cross-section") for scattering by N_2. In this and all subsequent data, the gas temperature was 298 K (1 eV = 1.602×10^{-19} J = 96.485 kJ mol^{-1}).

The motivation for our work has been to gain physical insight into the nature of the strongly quantum-dominated collisions of electrons with molecules in the thermal energy range between a few tens to a few thousand kelvin. Some parallel may be drawn between low-energy electron collisions and cold atom collisions: an electron with 10 meV energy, equivalent to a temperature of 115 K, has a wavelength of 122 Å (12.2 nm), which may be associated with a Rb atom at 5×10^{-4} K. In our electron scattering experiments, powerful quantum scattering effects are in evidence. These involve phenomena such as quantum interference and virtual state formation, revealing new and unexpected behavior.

Electron−molecule scattering was pioneered by Schulz[2,3] and has been intensively studied over a period of 30 years. In the realm of low-energy collisions, considerable early progress was made in the study of attachment of thermal electrons to molecules. Techniques avoided the use of electron beams and involved collisional ionization of high

David Field was born in Bristol, UK. He is currently a Professor of Physics at the University of Aarhus. He received his Ph.D. and Sc.D. from the University of Cambridge and worked at the University of Göttingen (1973−1975) and thereafter at the University of Bristol until 1999. His main interests are in electron−molecule collisions and observational and theoretical astrophysics.

Stuart Lunt was born in Cheshire, UK. He obtained his Ph.D. at the University of East Anglia. Between 1984 and 1997, he worked at Daresbury Synchrotron Radiation Laboratory and subsequently as a synchrotron radiation physicist at the University of Aarhus. In 2000, he joined Thermo VG Scientific as a senior development scientist.

Jean-Pierre Ziesel was born in the Berry region of France. He is currently Directeur de Recherche CNRS at the University Paul Sabatier at Toulouse. He worked for many years in the Laboratoire des Collisions Atomiques et Moléculaires at the University Paris-Sud at Orsay, moving recently to Toulouse. His main interests lie in electron scattering and in fast collisions of ions with surfaces.

* To whom correspondence should be addressed. E-mail: dfield@ifa.au.dk. Fax: +8612 0740. Tel.: +45 8942 3650.

10.1021/ar0000962 CCC: $20.00
Published on Web 02/10/2001

Rydberg state atoms,[4] electron-swarm methods[5] (for momentum transfer studies), flowing afterglow techniques,[6] and threshold photoionization of rare-gas atoms.[7] Related high-resolution laser photoionization work continues to yield exciting new results.[8] Species such as SF_6 or CCl_4[9,10] were found to have attachment cross-sections exceeding 1000 Å^2 (10^{-17} m^2) for electron energies of a few millielectronvolts.

Electron attachment is, however, only a subset of all scattering events that may occur when very low-energy electrons encounter molecules. Because of the technical difficulties associated with forming and controlling very low-energy electron beams,[11] the general field of electron scattering at thermal energies below, say, 100−200 meV, remained to a great extent unexplored until the advent of our experiments in the last 5−10 years. Some space is therefore devoted at first to a description of the techniques which we have developed to overcome these difficulties.

2. The Experimental Method

The present Account is limited to conceptually simple experiments in which electron beams are passed through target gases contained in gas cells at room temperature. The standard manner by which to create an electron beam with high energy resolution is to use a hot filament source in conjunction with electrostatic and magnetic fields. The highest energy resolution achieved lies between 10 and 20 meV and rapidly deteriorates to rarely better than 50 meV for electron energies below a few hundred millielectronvolts. Somewhat improved performance, for example 5 meV resolution at 250 meV energy, has been obtained using time-of-flight techniques[12] and in a pioneering photoionization source.[13] Surface science experiments may achieve ∼1 meV resolution in the analysis of photoelectrons under ultrahigh-vacuum conditions,[14] but no attempt has been made to perform the formidable task of turning the experiment around, as it were, and performing gas-phase scattering experiments using the most recent surface science techniques. Here and subsequently, resolution is quoted in terms of full-width at half-maximum of an assumed Gaussian energy distribution.

In our work, a synchrotron radiation photoionization technique is used to create the electrons which are then used for scattering experiments. Figure 2 shows a scale diagram of the apparatus. The heart of the apparatus is a cell in the center of which synchrotron radiation is focused to a strip of thickness of 10 μm or less. Electrons are formed by photoionization of Ar, at a pressure of a few tens of millipascal, using radiation tuned to 78.65 nm, ∼4 meV above the threshold for Ar photoionization. The energy resolution of the electrons is determined by the energy resolution of the photon beam. In the course of our recent work we have used three different synchrotron sources, SuperACO at LURE, Université Paris-Sud, the Daresbury Synchrotron Radiation Source, UK, and presently the ASTRID source at the University of Aarhus, Denmark. The energy resolution in the ionizing photon beam has varied between 5 and 6 meV to a present typical

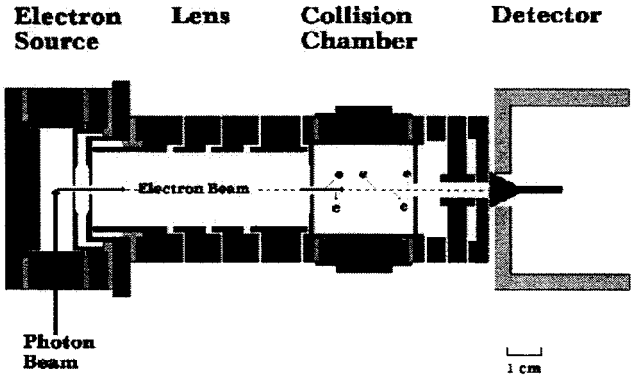

FIGURE 2. Schematic diagram of the apparatus used to obtain data shown in this article. A monochromatic synchrotron photon beam at 78.65 nm issues from the exit slit of a monochromator, for example the 5-m McPherson at the SRS, Daresbury Laboratory, or the spherical grating monochromator on the undulator beam line at ASTRID, Aarhus. The photon beam is focused into a cell containing argon, yielding photoelectrons of a few millielectronvolts energy. Electrons are continuously expelled from the region of formation and formed into a beam with an electrostatic lens. Cross-sections are measured by recording the attenuation of the electron beam as it traverses the collision chamber containing the target gas.

figure using the ASTRID undulator beamline of 0.95 meV, with a number of experiments performed at 0.75 meV resolution.

An electric field of 0.2−0.4 V/cm in the region of photoionization draws the low-energy electrons out of the source, forming a focused beam with the four-element electrostatic lens shown in Figure 2. The electric field in the photoionization electron source is too weak to degrade the electron energy resolution significantly. The electron beam passes through a cell containing the target gas. The beam attenuation as a function of electron energy is measured by recording the electron current on a channel electron multiplier situated beyond various further optical elements. The electron energy is scanned by varying the potential in the photoionization source. The whole apparatus can be immersed in an axial magnetic field, which is typically set to 20 G.[15]

Absolute cross-sections are evaluated using

$$I_t = I_0 \exp(-\sigma N z)$$

where I_t and I_0 are the attenuated and unattenuated electron currents, respectively, σ is the scattering cross-section for any chosen electron energy, N is the target gas number density, and z is the effective electron path length in the target gas. Measurement of pressure is a decisive factor in the absolute accuracy of our measured cross-sections. Presently, a Leybold rotating ball gauge (Viscovac VM212) is used. A further source of error may lie in the value of the effective path length of electrons in the gas. Detailed tests using He and N_2 show that the geometrical length of the collision path (30 mm) is, within experimental error, the true effective length. Numerous comparisons with data obtained in other laboratories show that good agreement may be achieved for absolute values of cross-sections. Across the board, the level of agreement is

generally ±10%, sometimes rather better, between results from different laboratories.

In the absence of an axial magnetic field, the measured cross-section is the total integral scattering cross-section, where "total" refers to all elastic and inelastic events and "integral" refers to integration over the full 4π solid angle. When the magnetic field is present, electrons form a tightly confined beam and spiral around the axial direction of the field. When electrons are scattered by the target gas, those that are directed into the forward hemisphere are picked up by the magnetic field and continue along an axial path. These electrons exit the scattering cell and are detected as unscattered. Electrons which are scattered into the backward hemisphere are again picked up by the magnetic field, retrace their paths backwards through the apparatus, and are lost in the vicinity of the source region. Thus, in the presence of the magnetic field, the measured cross-section is a total backward-scattering cross-section, that is, a cross-section integrated over the 2π steradian solid angle associated with the backward hemisphere.[16]

Measurements of backward-scattering cross-sections are limited to energies below 650 meV. This arises because electrons which have a transverse component of energy exceeding ~650 meV, acquired through a collision, cannot pass through the 3-mm-diameter exit hole of the target cell in the presence of a 20-G axial magnetic field. Thus, above an impact energy of 650 meV, forward scattering will contribute to the measured cross-section. This behavior has been rigorously checked by comparison with data for N_2 measured by other groups, e.g., ref 17.

To tune the electron energy, the target chamber is held at 0 V, and voltages are set on the photoionization chamber such that electrons are formed at a potential of, say, −0.5 V. However, the electron energy at the target will not then be precisely 0.5 eV, since contact potentials, for example, may introduce shifts of several tens of millielectronvolts or more. Fortunately, electron energies have been unequivocally measured through time-of-flight for scattering by N_2[18] and O_2.[19,20] For example, the energy of the third peak in the N_2 spectrum in Figure 1 has been determined to be 2.442 ± 0.015 eV[18] and is moreover insensitive to the angle of observation. Using these and other data,[16] the absolute energy scale can be specified with an uncertainty of typically ±5 meV.

Over a period of years, we have investigated the low-energy electron scattering characteristics of 60 or more target species. A few of our results, selected from more recent data, will be used here to illustrate elastic scattering, rotationally inelastic scattering, virtual state formation, and quantum interference phenomena.

3. Elastic Scattering

Collisions are described in the classical picture by particles moving in their mutual force field. At long range, the electron−atom or electron−molecule potential is well-characterized by a charge−induced dipole interaction. This yields a potential proportional to the electric dipole polarizability of the target divided by the electron−target distance to the fourth power. At closer range, description of the interaction requires a detailed treatment of correlation and exchange. Electron correlation describes how the motion of one or more electrons, in particular the impacting electron, affects the motions of other electrons within a target molecule. The purely quantum mechanical phenomenon of electron exchange describes how, as the collision progresses, the impacting electron loses its identity as a particle separate from the target electrons. The exchange integral is larger for lower total energies of the system and therefore becomes increasingly important for lower electron impact energy. For low-energy encounters, one can no longer use the concept of a potential surface, familiar from heavy particle collisions. A description of the composite system for low collision energy is given rather by the wave function for all electrons in the system including the impacting electron.

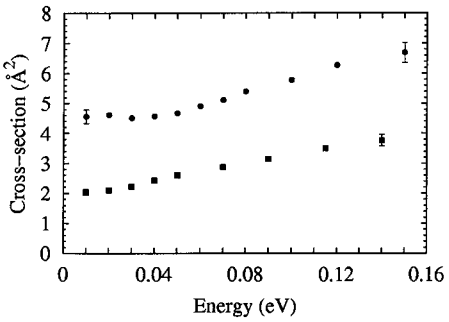

FIGURE 3. Variation with electron energy of the electron-scattering cross-section integrated over the backward hemisphere for all elastic and inelastic processes (the "total backward cross-section") for scattering by H_2 (upper set) and N_2 (lower set).[16]

The value of the cross-section for scattering at low energies depends on the detailed form of the wave function for this negative molecular composite. It follows that the low-energy variation of the scattering cross-section differs very greatly in classical and quantum descriptions. In classical physics, the value of the cross-section is proportional to $(\alpha/E)^{1/2}$, where α is the target electric dipole polarizability and E the collision energy. Thus, as the electron impact energy approaches zero, the scattering cross-section should rise toward infinity. Quantum mechanics dictates, however, that the cross-section achieves a finite and usually rather small value at very low electron collision energies, with the value becoming increasingly energy independent with lower collision energy. Figure 3 shows values of total backward-scattering cross-section for both N_2 and H_2 between 10 and 150 meV electron impact energy.[16] These data exemplify quantum scattering. Note that the scattering cross-section for H_2 is more than twice as large as that for N_2 at 10 meV, although the polarizability of H_2 is less than half that of N_2. Cross sections for rotationally inelastic scattering are small for molecules without a permanent dipole moment, and therefore the data in Figure 3 represent almost entirely elastic scattering.

Electron scattering by benzene should show behavior similar to that found in Figure 3, since benzene, like N_2 or H_2, has no dipole moment (or sufficiently low lying

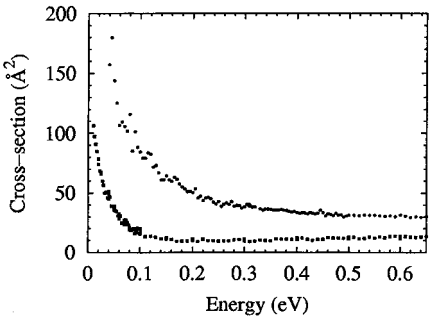

FIGURE 4. Variation with electron energy of the total integral electron-scattering cross-section (upper set) and total backward-scattering cross-section for perdeuterated benzene, C_6D_6.

vibrational modes) and thus no energetically open channels for strong inelastic scattering at very low energy. However, benzene shows behavior strikingly different from that of N_2 and H_2, with a cross-section rising rapidly at very low energy. This is shown in Figure 4 for C_6D_6 for both integral and backward scattering.[15]

To progress in our understanding of the data in Figures 3 and 4, we attempt to visualize the nature of an incoming electron wave, from a viewpoint standing on the target molecule. Because an electron is spread out in space, an incoming wave is a superposition of states, rather than a classical state of precisely defined trajectory. To each state within this superposition may be accorded a certain quantized collisional angular momentum with respect to the target, each component state being assigned a quantum number l. By analogy with the hydrogen atom, $l = 0$ components are called s-waves, $l = 1$ p-waves, $l = 2$ d-waves, etc., where the l components are collectively called "partial waves". The angular distribution of scattered electrons associated with individual partial waves follows the mathematical form associated with s-, p-, and d-orbitals, etc.

If an electron wave passes close to the target, low angular momentum components dominate; if the electron wave passes far from the target, high angular momentum states dominate. Since electrons are very light, at low collision energies of tens of millielectronvolts, high angular momentum states will tend to be concentrated at large distances from the target, for example at several nanometers from the scattering center. Low angular momentum states will, by contrast, represent near head-on impacts, to use a classical analogy. Thus, high angular momentum components interact weakly, and low angular momentum states interact relatively strongly. At low impact energy, very few partial waves may be involved in scattering, allowing for detailed insight into the nature of the collisions.

As component partial waves are scattered, deviate from their initial direction, and depart from the target, they undergo a shift of phase as they spread out in space. The extent of the phase shift is a measure of the strength of the interaction between the wave and the target. Theory shows that the cross-section for scattering is proportional to sine-squared of the phase shift (for a spherically symmetric force field—obviously an approximation here). From the data in Figure 3, we can deduce, for example, that for H_2 the incoming s-wave, when scattered, undergoes a phase shift of absolute value 0.103 rad (mod π), or $\sim 6°$, at an impact energy of 20 meV. Moreover, this component of the wave will be scattered with an angular distribution which is spherical, in keeping with s-wave character. The target may also select the p-wave component of the superposition of s- and p- states of the incoming electron wave. This component, with an experimental phase shift 0.071 rad, will be scattered with backward–forward asymmetry, characteristic of a p-wave. To a good approximation, angular momentum waves higher than p-waves interact too weakly to make a significant contribution. The overall angular distribution of scattered electrons represents that of a superposition of s- and p-waves. Experimentally, the angular distribution shows 60% scattered into the backward hemisphere and 40% into the forward at 20 meV impact energy. Thus, the superposition of outgoing scattered waves represented by $s - p$ is favored over that represented by $s + p$. This reflects the intuition that low-energy waves will tend to be more readily deflected into the backward hemisphere on encountering a massive obstacle, such as H_2, rather than scattered into the forward hemisphere.

What then of the behavior of benzene, shown in Figure 4 to exhibit behavior quite different from that of H_2 or N_2? In this case, a new quantum phenomenon is at play, the formation of a so-called "virtual state". A physical description of virtual state scattering is as follows. The electron–benzene interaction yields an energy well with which may be associated states of $(benzene)^-$. Depending on the strength of the interaction, such states may, in principle, be bound or lie in the continuum, a little above the top of the well. The latter give rise to virtual state scattering, in which a bound state of the electron and benzene is almost, but not quite, born. If such a state in the continuum differs by an energy ΔE from the energy of the incoming electron, then for a time Δt, determined by the Heisenberg relationship $\Delta E \Delta t \geq h/2\pi$, the electron wave in the presence of benzene feels the influence of the state for the brief period Δt. The presence of the state in the continuum gives an additional phase shift to the scattered electron wave. The smaller the energy mismatch, ΔE, the greater is the cross-section in the limit of low energy. Virtual state scattering does not lengthen the lifetime of the electron–molecule encounter and is therefore not resonant scattering. Moreover, only s-waves give rise to the virtual state effect, which has the characteristic that the scattering cross-section peaks as the impact energy approaches zero. If higher angular momentum waves are involved, shape resonances, for example, could be formed above zero energy, involving states of $(benzene)^-$ in the continuum (though in fact we see no evidence for these). Since only s-waves are involved in virtual state scattering, the scattering cross-sections should become backward–forward symmetric at the lowest impact energies. The ratio of the backward to the integral scattering cross-section for C_6D_6 is plotted in Figure 5. Results are consistent with a ratio of ~ 0.5 close to zero electron

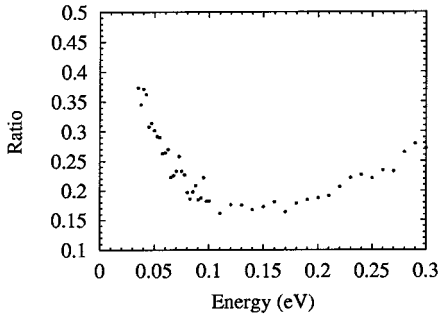

FIGURE 5. Variation with electron energy of the ratio of the backward to the integral scattering cross-sections for C_6D_6, obtained from data in Figure 4.

impact energy, corresponding to the requisite backward−forward symmetry of s-wave-dominated scattering. Concurrently with our experiments,[15] theoretical work was in progress which predicted the formation of a virtual state in electron scattering by benzene.[21] Characteristics predicted by theory, if not precise cross-sections, turned out to be those which we observed in the laboratory.

We have observed electron-scattering behavior similar to that in benzene for larger aromatics without dipole moments, such as naphthalene, anthracene, and perylene. We suspect, therefore, that virtual states may be common among large nonpolar (or weakly polar) but polarizable species, such as those with conjugated aromatic systems. Very recently, experiments have been performed with CO_2, which has been postulated to show virtual state formation.[22,23] Our data show the first prima facie evidence for the existence of a virtual state in any molecule, where measurements extend down to collision energies of ∼7 meV for both integral and backward-scattering cross-sections. The integral scattering cross-section at this energy is ∼135 Å^2, and the backward-scattering cross-section is a little less than half this value. Detailed analysis confirms the s-wave nature of the interaction which, as we seen above, is an essential feature of virtual state scattering.

4. Rotationally Inelastic Scattering

Molecular targets have so far been limited to species with no permanent dipole moment. For a molecule with a dipole moment, the interaction with a charge follows an inverse square law with distance rather than an inverse fourth power. The long range of the inverse square law interaction has important consequences for low-energy collisions. Note that the passage of an electron with, say, 10 meV energy takes no more than a few hundredths of a picosecond, a period of time over which molecules at room temperature barely perform any rotational motion. Thus, for a polar target, the dipole seen by the incoming electron is approximately frozen in space.

The long range of the electron−dipole interaction has the effect that even those waves which are at very large impact parameters, that is, high l waves, are pulled in toward the target molecule. Theory[3] predicted correspondingly high cross-sections, so high in fact that for molecules with dipole moments of more than 0.1−0.2 D, elastic events should, in general, be negligible by comparison with rotationally inelastic events. Theory remained, however, untested until we first detected rotationally inelastic scattering near threshold in the chlorofluorohydrocarbons ("freons")[24] and in subsequent experiments measured absolute scattering cross-sections, for example for the halobenzenes.[25] Theory rests on the basis of a model in which any partial wave interacts through a dipolar force to cause the state of the target to change from an initial rotational state to a final rotational state, without the involvement of any other rotational states. This "first-order" approximation constrains transitions to follow standard dipole selection rules for rotational transitions. The probability of the transition induced by electron impact is therefore related directly to the line strength of the allowed dipole transition. In this model, only one unit of angular momentum may be transferred in the collision. Evidently, if high angular momentum waves are involved, the velocity vector of the electron changes direction very little for the exchange of a single rotational quantum, and the wave is strongly forward scattered. While in some collisions low angular momentum waves will enhance higher angle scattering, theory predicts overall strong forward scattering. In addition, according to the model, the cross-section depends inversely on the electron impact energy, with a weak logarithmic modification involving the energies of incoming and outgoing electron waves.

It is of considerable practical importance to test the predictive power of this model, embodied in the so-called "first-order Born point-dipole" theory. Results obtained with Born theory are generally all that are available for modeling plasmas for deposition and reactive ion and plasma etching. Thermalization of electrons in plasmas containing polar gases determines the important parameter of effective electron temperature[26,27] and is strongly influenced by the very rapid processes of rotation−translation energy transfer which Born theory predicts. Cooling of electrons through inelastic collisions is also important in astrophysical plasmas. The high abundance of polar species such as water or ammonia forms populations of electrons thermalized to the rotational temperature of molecules in interstellar clouds. In both natural and man-made plasmas, cold electrons may then go on to attach with high efficiency to large molecules, for example to polycyclic aromatic hydrocarbons in the interstellar medium. The results obtained in the field of rotationally inelastic scattering are therefore of interest both for the light they shed on the nature of the process of energy transfer and for affording some measure of respectability, or otherwise, to cross-sections estimated using the simple-to-apply Born theoretical model.

How, then, do the predictions of theory compare with our experimental data? In our first observations of low-energy rotationally inelastic scattering (in freons),[24] it was apparent that very large scattering cross-sections are found at low impact energies as theory demanded. Subsequently, values have been measured exceeding 1000 Å^2 in numerous species with large dipole moments such

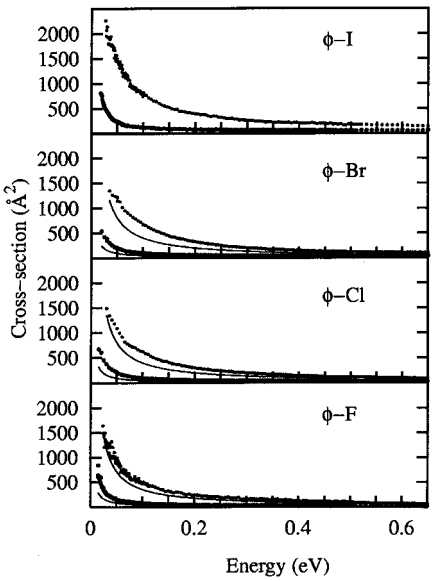

FIGURE 6. Variation with electron energy of the total integral electron-scattering cross-section (upper set in each frame) and total backward-scattering cross-section (lower set in each frame) for the four halobenzenes.[25] The continuous lines show cross-sections calculated using Born theory, see section 4.

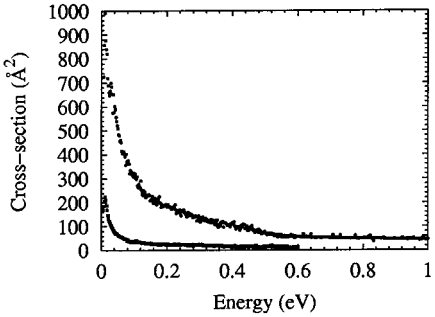

FIGURE 7. Variation with electron energy of the total integral electron-scattering cross-section (upper set) and total backward-scattering cross-section (lower set) for methanol. These data were obtained with an energy resolution in the electron beam of 0.75 meV.

as halobenzenes,[25] nitromethane,[28] etc. We have also verified the theoretical prediction that scattering should be strongly in the forward direction. The experimental results shown in Figure 6 for the halobenzenes, with dipole moments of between 1.6 and 1.7 D, illustrate both the very large cross-sections involved and strong forward scattering. Further data are shown in Figure 7 for methanol, with a dipole moment along the principal axis of 1.7 D.

Quantitative comparison with theory presents a less rosy picture, especially in the energy regime below ~200 meV. Born calculations are erratic in reproducing the experimental data, showing underestimates (for halobenzenes,[25] Figure 6) and overestimates (for ozone,[29] Figure 8) of both the integral and backward-scattering cross-sections. Errors may exceed a factor of 2, for example for ozone around 10 meV electron impact energy, although much better agreement may sometimes be found, as for fluorobenzene in Figure 6.

There is a clear general trend that the Born model increasingly overestimates the degree of forward scattering as the electron energy decreases. At low energy, the approximation that higher partial waves dominate the scattering is less tenable. Despite the long-range nature of the electron−dipole interaction, at low enough energy higher partial waves cease to contribute strongly to the scattering, and fewer partial waves with greater phase shifts and larger scattering angles must contribute more strongly. Our results show that this begins to be important below 100−200 meV impact energy. We conclude that above a few hundred millielectronvolts, standard Born theory may be used with reasonable confidence to provide data for plasma modeling. If, however, the low-temperature electron distribution is critical to plasma properties—which it may well be for electronegative plasmas in device manufacture and most certainly is for the interstellar medium—then experimental values should be sought or theorists should be prevailed upon to improve their estimates. To complicate the issue, there appears to be a significant class of molecules which show behavior, at low electron impact energy, almost entirely at odds with the predictions of the Born model. It is to these interesting species which we now turn.

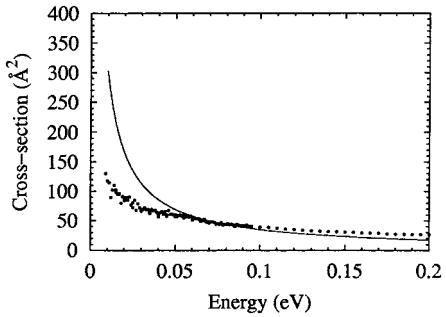

FIGURE 8. Variation with electron energy of the total integral electron-scattering cross-section for ozone.[29] The continuous line shows cross-sections calculated using Born theory, see section 4.

5. Interference Phenomena and the Suppression of Rotational Energy Transfer

When electrons impact on nitromethane[28] at 100 meV, the integral cross-section for rotationally inelastic scattering is ~1100 Å². The dipole moment of nitromethane is 3.46 D. When the same experiment is performed using nitrobenzene as a target, the cross-section is ~70 Å². The dipole moment of nitrobenzene is 4.23 D, and a crude estimate of the scattering cross-section would suggest that it would be $(4.23/3.46)^2 \approx 1.5$ times greater than that for nitromethane, that is, around 1650 Å² or ~25 times more than that observed at 100 meV. The scattering spectrum for nitrobenzene[28] for both integral and backward-scattering is shown in Figure 9. Qualitatively similar behavior has been found in chlorine dioxide[30] (Figure 10), in Cl_2O, and in CF_3Cl (Freon-13). Figures 9 and 10 show a quite unexpected suppression of rotationally inelastic scattering for certain ranges of electron impact energy. At higher energies, the Born model may be moderately satisfactory, for example overestimating the integral scattering cross-section by ~60% for nitrobenzene at 300 meV and

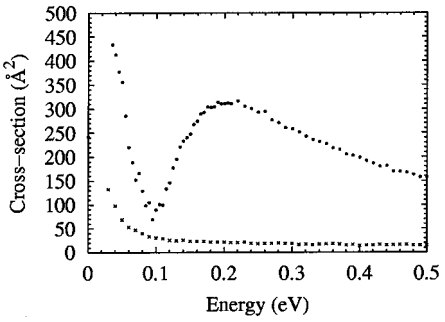

FIGURE 9. Variation with electron energy of the total integral electron-scattering cross-section (upper set) and total backward-scattering cross-section (lower set) for nitrobenzene.[28]

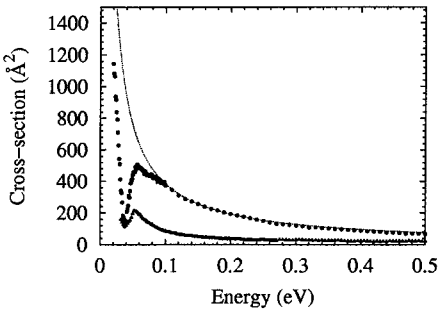

FIGURE 10. Variation with electron energy of the total integral electron-scattering cross-section (upper set) and total backward-scattering cross-section (lower set) for chlorine dioxide. The thin dotted line shows total integral cross-sections calculated using Born theory, see sections 4 and 5.

providing an accurate estimate down to 100 meV impact energy for ClO_2 (Figure 10). On the basis of our present results involving only four different species, we cannot predict which molecules may behave in the manner shown in Figures 9 and 10.

The suppression of rotational excitation presumably arises through an interference phenomenon in which incoming and outgoing partial waves, scattered through rotationally inelastic events, interfere destructively. This must involve many partial waves, with high l waves dominant, since structure is either much weaker (ClO_2) or absent (nitrobenzene, CF_3Cl) in the backward-scattering cross-section. Suppression of rotationally inelastic scattering, however, remains present in backward-scattering events.

We tentatively suggest the following. There exist states of the target negative ion, accessible over a range of energies, for which the probability of formation peaks where rotationally inelastic scattering is most strongly suppressed. The energies of these states correspond to energies of the LUMOs, associated with nuclear configurations which are largely unchanged from those of the neutral. These "temporary negative ion" states constitute resonant scattering states. Any such state may decay rapidly into a free scattered electron and target molecule. In the interaction of the electron waves with the polar species, there are therefore two channels open to the electron, direct Born-type rotational scattering or scattering via a negative ion state. Quantum theory requires that the electron explore both of these in superposition. The two paths therefore interfere, apparently destructively. An analogy may be made with the well-known interference phenomenon giving rise to so-called Fano line shapes in photoabsorption above the ionization continuum. In this case, highly excited states of the target may be accessed by absorption of photons with energies above the ionization potential. Ionization at appropriate wavelengths takes place through a superposition of direct ionization and indirect ionization via the bound state in the continuum, with accompanying interference between these channels.

6. Concluding Comments

Results described here show how quantum phenomena dominate low-energy electron scattering. Concepts such as the quantization of collisional angular momentum and matter wave interference are essential in order to interpret the variation of scattering cross-section with electron impact energy and the elastic and inelastic events which accompany electron−molecule encounters in the thermal energy region.

Drawing on our data as a whole, we have learned that the first-order Born point-dipole approximation is a somewhat wayward device for the calculation of rotationally inelastic scattering cross-sections. Cross sections may be higher or lower than Born predicts in the thermal energy region, and further theoretical work is necessary in this area. We have moreover encountered a class of species, of disparate chemical nature, whose low-energy scattering behavior is highly discrepant with the predictions of any existing theory. It is not possible at present to predict which species are likely to show the striking phenomena, attributed to interference, which we have observed, for example, in Freon-13 (CF_3Cl) or nitrobenzene. Additionally, the formation of virtual states may be a rather general phenomenon among larger molecular species, viz. data for naphthalene, anthracene, and perylene mentioned above. Virtual states may act as gateways for the formation of stable negative ions through intersystem crossing and internal conversion, a feature of interest in man-made plasmas, in combustion, in the atmospheres of the earth and other planets, and in the interstellar medium.

We thank the Directors and staff of Daresbury Laboratory, LURE (Université of Paris-Sud), and the Institute of Synchrotron Radiation at Aarhus (ISA) for providing access to the SRS, Super-ACO, and ASTRID. We also thank the EPSRC (UK), the Royal Society, the CNRS, and the Danish National Science Foundation for financial support.

References

(1) Boudaïffa, B.; Cloutier, P.; Hunting, D.; Huels, M. A.; Sanche, L. Resonant Formation of DNA Strand Breaks by Low-Energy (3 to 20 eV) Electrons. *Science* **2000**, *287*, 1658.
(2) (a) Schulz, G. J. Resonances in electron impact on diatomic molecules. *Rev. Mod. Phys.* **1973**, *45*, 423. (b) Schulz, G. J. In *Principles of Laser Plasmas*; Bekefi, G. Ed.; Interscience: New York, 1976; Chapter II.
(3) Shimamura, I.; Takayanagi, K. *Electron−Molecule Collisions*; Plenum: New York, 1984.

(4) Foltz, G. W.; Latimer, C. J.; Hildebrandt, G. F.; Kellert, F. G.; Smith, K. A.; West, W. P.; Dunning, F. B.; Stebbings, R. F. Ionization of xenon atoms in high Rydberg states by collision with molecules. *J. Chem. Phys.* **1977**, *67*, 1352.
(5) Christodoulides, A. A.; Christophorou, L. G.. Electron attachment to brominated aliphatic hydrocarbons of the form n-$C_NH_{2N+1}Br$ (N = 1−6, 8, and 10). I. An electron swarm study. *J. Chem. Phys.* **1971**, *54*, 4691.
(6) Smith, D.; Adams, N. G.; Alge A. Attachment coefficients for the reactions of electrons with CCl_4, CCl_3F, CCl_2F_2, $CHCl_3$, Cl_2 and SF_6 determined between 200 and 600 K using the FALP technique. *J. Phys. B* **1984**, *17*, 461.
(7) Ajello, J. M.; Chutjian A. Line shapes for attachment of threshold electrons to SF_6 and $CFCl_3$. Threshold photoelectron (TPSA) studies of Xe, CO, and C_2H_2. *J. Chem. Phys.* **1979**, *71*, 1079.
(8) Schramm, A.; Fabrikant, I. I.; Weber, J. M.; Leber, E.; Ruf, M.-W.; Hotop, H. Vibrational resonance and threshold effects in inelastic electron collisions with methyl iodide molecules. *J. Phys. B: At. Mol. Opt. Phys.* **1999**, *32*, 2153.
(9) Chutjian, A.; Alajajian, S. H. s-wave threshold in electron attachment: observations and cross sections in CCl_4 and SF_6 at ultralow electron energies. *Phys. Rev. A* **1985**, *31*, 2885.
(10) Randell, J.; Field, D.; Lunt, S. L.; Mrotzek, G.; Ziesel, J.-P. Low-energy electron scattering by SF_6. *J. Phys. B: At. Mol. Opt. Phys.* **1992**, *25*, 2899.
(11) Field, D.; Knight, D. W.; Mrotzek, G.; Randell, J.; Lunt, S. L.; Ozenne, J.-B.; Ziesel, J.-P. A high-resolution synchrotron photoionization spectrometer for the study of low-energy electron−molecule scattering. *Meas. Sci. Technol.* **1991**, *2*, 757.
(12) Ferch, J.; Raith, W.; Schröder, K. Total cross section measurements for electron scattering from molecular hydrogen at very low energies. *J. Phys. B: At. Mol. Phys.* **1980**, *13*, 1481.
(13) Gallagher A.; York, G. A photoionization source of monoenergetic electrons. *Rev. Sci. Instrum.* **1974**, *45*, 662.
(14) Ibach, H. *Electron Energy Loss Spectrometers*; Springer: 1991.
(15) Gulley, R. J.; Lunt, S. L.; Ziesel, J.-P.; Field, D. Very low energy electron scattering from benzene and deuterated benzenes. *J. Phys. B: At. Mol. Opt. Phys.* **1998**, *31*, 2735.
(16) Randell, J.; Lunt, S. L.; Mrotzek, G.; Ziesel, J.-P.;Field, D. Low energy electron scattering in H_2, N_2 and O_2. *J. Phys. B: At. Mol. Opt. Phys.* **1994**, *27*, 2369.
(17) Sun, W.; Morrison, M. A.; Isaacs, W. A.; Trail, W. K.; Alle, D. T.; Gulley, R. J.; Brennan, M. J.; Buckman, S. J. Detailed theoretical and experimental analysis of low-energy electron-N_2 scattering. *Phys. Rev. A* **1995**, *52*, 1229.
(18) Kennerly, R. E. Absolute total electron scattering cross sections for N_2 between 0.5 and 50 eV. *Phys. Rev. A* **1980**, *21*, 1876.
(19) Land, J. E.; Raith, W. High-resolution measurement of resonances in e-O_2 scattering by electron time-of-flight spectroscopy. *Phys. Rev. A* **1974**, *9*, 1592.
(20) Field, D.; Mrotzek, G.; Knight, D. W.; Lunt, S. L.; Ziesel, J.-P. High-resolution studies of electron scattering by molecular oxygen. *J. Phys. B: At. Mol. Opt. Phys.* **1988**, *21*, 171.
(21) Gianturco, F. A.; Lucchese R. R. One-electron resonances and computed cross sections in electron scattering from the benzene molecule. *J. Chem. Phys.* **1998**, *108*, 6144.
(22) Morrison, M. A. Interpretation of the near-threshold behaviour of cross-sections for e-CO_2 scattering. *Phys. Rev. A* **1982**, *25*, 1445.
(23) Morgan, L. A. Virtual states and resonances in electron scattering by CO_2. *Phys. Rev. Lett.* **1998**, *80*, 1873.
(24) Randell, J.; Ziesel, J.-P.; Lunt, S. L.; Mrotzek, G.; Field, D. Low energy electron scattering by CF_3Cl, CF_2Cl_2, $CFCl_3$ and CCl_4. *J. Phys. B: At. Mol. Opt. Phys.* **1993**, *26*, 3423.
(25) Lunt, S. L.; Field, D.; Hoffmann, S. V.; Gulley, R. G.; Ziesel, J.-P. Very low energy electron scattering in C_6H_5F, C_6H_5Cl, C_6H_5Br and C_6H_5I. *J. Phys. B: At. Mol. Opt. Phys.* **1999**, *32*, 2707.
(26) Chapman, B. N. *Glow Discharge Processes*; Wiley: New York, 1980.
(27) May, P. W.; Klemperer D. F.; Field, D. Monte Carlo simulations of electron distributions in the sheath region of reactive-ion-etching plasmas. *J. Appl. Phys.* **1993**, *73*, 1634.
(28) Lunt, S. L.; Field, D.; Ziesel, J.-P.; Jones, N. C.; Gulley, R. G. Very low energy electron scattering in nitromethane, nitroethane and nitrobenzene. *Int. J. Mass Spectrom.,* **2001**, in press.
(29) Gulley, R. G.; Field, T. A.; Steer, W. A.; Mason, N. J.; Lunt, S. L.; Ziesel, J.-P.; Field, D. Electron scattering in ozone and chlorine dioxide. *J. Phys. B: At. Mol. Opt. Phys.* **1998**, *31*, 5197.
(30) Field, D.; Jones, N. C.; Gingell J. M.; Mason, N. J.; Lunt, S. L.; Ziesel, J.-P. Electron scattering in chlorine dioxide. *J. Phys. B: At. Mol. Opt. Phys.* **2000**, *33*, 1039.

AR0000962